Supporting Information for:

Turbine-like Structured Silica Transcribed Simply by Pre-structured Crystallites of Linear Poly(Ethyleneimine) Bounded with Metal Ions

Hiroyuki Matsukizono[a], Pei-Xin Zhu[a], Norimasa Fukazawa, Ren-Hua Jin*[a, b]

a) Synthetic Chemistry Laboratory, Kawamura Institute of Chemical Research, and b) JST-CREST, 631 Sakado, Sakura, Chiba 285-0078, Japan.

E-mail: jin@kicr.or.jp

1. Absorption spectra of LPEI/M^{II}(p-$TolSO_3$)$_2$ solutions (M = Ni, Cu)

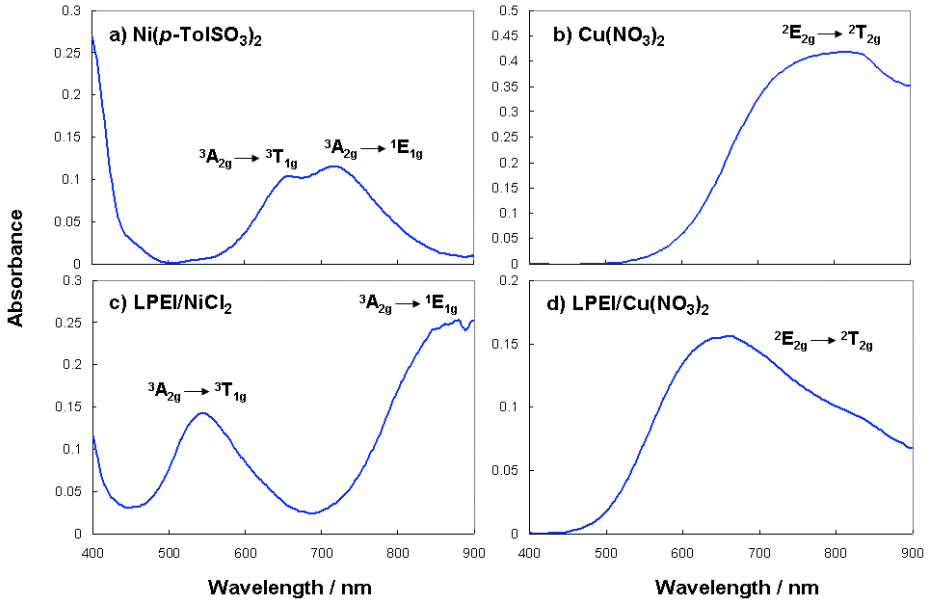

Figure S1. Absorption spectra in water. a) Ni(p-$TolSO_3$)$_2$ solution. b) $Cu(NO_3)_2$ solution, [Cu] = 10 mM. c) LPEI/$NiCl_2$ solution. d) LPEI/$Cu(NO_3)_2$ solution, [Cu] = 1 mM, [EI] = 6 mM.

Figure S1a) and b) display absorption spectra of M^{II}(p-$TolSO_3$)$_2$ solutions (M = Ni, Cu). In Figure S1a), two absorptions were observed at 550-650 nm, which are described to the d-d transitions ($^3A_{2g}\rightarrow{}^3T_{1g}$ and $^3A_{2g}\rightarrow{}^1E_{1g}$) of Ni^{II} complexes in the O_h symmetry. These absorptions indicate the coordination of Ni^{II} ion with six water molecules.[9a] In Cu^{II} solution, a broad absorption at 800 nm was observed. Similar to Ni^{II} solution, this absorption arises from the d-d transition of Cu^{II} aqua complex ($^2E_{2g}\rightarrow{}^2T_{2g}$). Generally, d-d transitions shift and/or split after conversions of coordinating ligands. When LPEI are added to these Ni^{II} or Cu^{II} solutions, their spectra were changed. Figure S1c) shows two large peaks at 540 and above 800 nm, which is typically observed in Ni^{II} ions coordinated with six amine ligands.[1] Therefore, it is obvious that amine groups of LPEI coordinate with metal ions instead of water molecules.

2. XRD charts of precipitates formed in LPEI/metal salts aqueous solutions

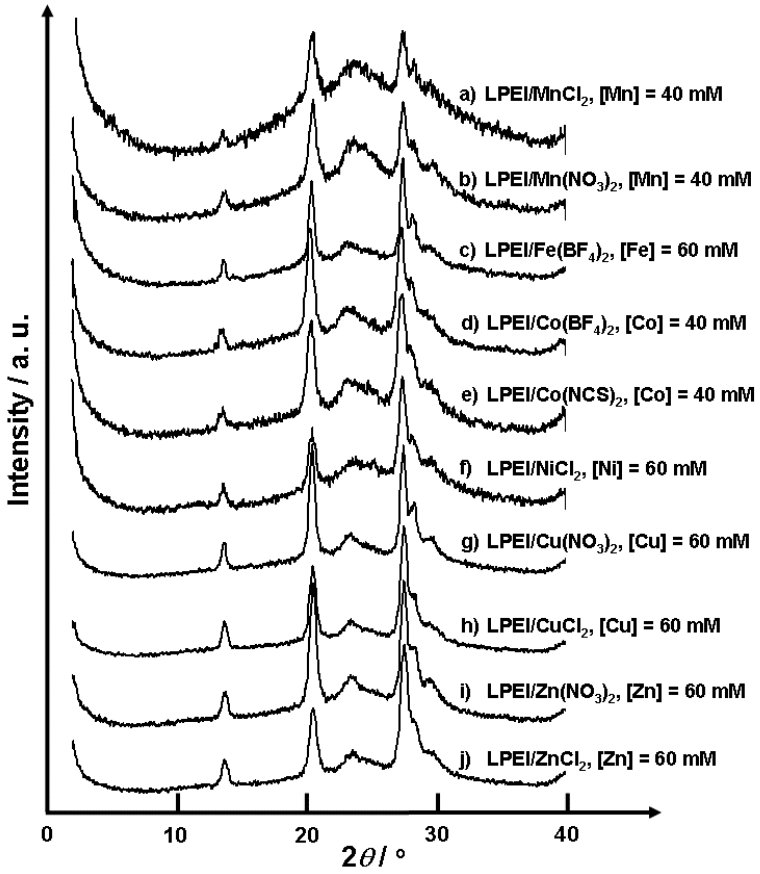

Fig. S2 XRD profiles of precipitates formed from LPEI aqueous solution containing a various metal salts. a) $MnCl_2$, b) $Mn(NO_3)_2$, c) $Fe(BF_4)_2$, d) $Co(BF_4)_2$, e) $Co(NCS)_2$, f) $NiCl_2$, g) $Cu(NO_3)_2$, h) $CuCl_2$, i) $Zn(NO_3)_2$, j) $ZnCl_2$. [EI] = 1000 mM. [M] = 40 or 60 mM.

Figure S2 shows XRD profiles of precipitates formed in LPEI aqueous solutions containing a wide variety of metal salts. Irrespective of different concentration and combination between metal ions and counter ions, all precipitates show four diffraction peaks with at 2θ = 14, 21, 27 and 28°. This pattern is characteristic for hydrated LPEI (H_2O/EI = 2). These suggest the uniformity of the role of metal salts used in this experiment on the aggregation of LPEI.

3. FT-IR spectra of precipitates formed from LPEI/$M^{II}(SCN)_2$ (M = Ni, Cu) aqueous solutions

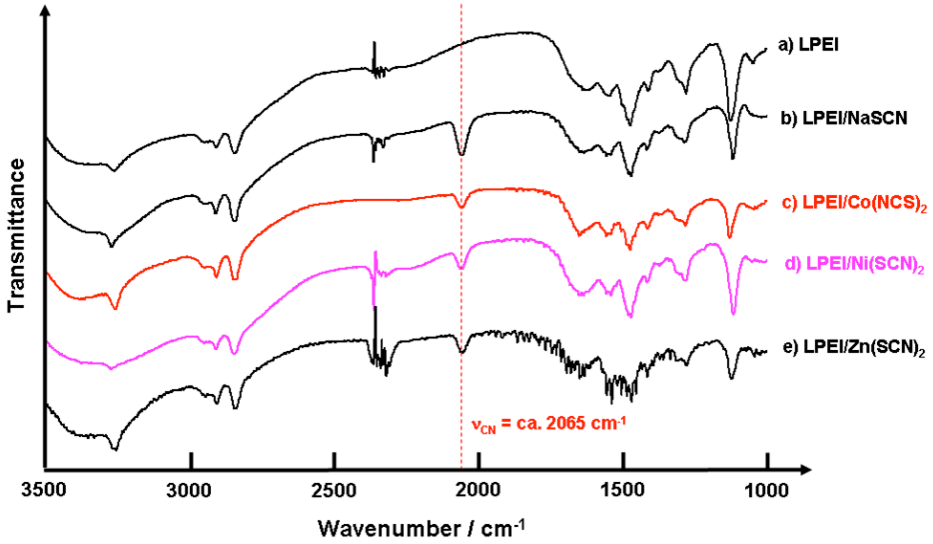

Fig. S3 FT-IR spectra of the aggregates composed of LPEI/$M^{II}(SCN)_2$. Each spectrum stands for the aggregates formed from LPEI (a), LPEI/NaSCN (b), LPEI/$Co(NCS)_2$ (c), LPEI/$Ni(SCN)_2$ (d), LPEI/$Zn(SCN)_2$ (e).

Figure S3 shows FT-IR spectra from 3500 to 1000 cm^{-1} of LPEI/$M^{II}(SCN)_2$ (M = Co, Ni, Zn). To observe the vibrations clearly, no silicified samples were subjected to measurements. FT-IR spectra of LPEI and LPEI/NaSCN are also exhibited in the figure. In all figures, three absorptions are observed at 3300, 2900, 2800 cm^{-1}, which characterize the stretching vibrations of secondary amine (N-H), asymmetric and symmetric methylene (C-H) vibrations, respectively. Except the spectrum of LPEI, there is one vibration at 2065 cm^{-1} in other samples, which is the characteristic CN stretching vibration for thiocyante ions. It has been reported that CN stretching vibrations located at ca. 2060 cm^{-1} is caused by contact ion pairs and/or solvent-separated dimmers of NaSCN in polyethyleneoxides.[2] Indeed, LPEI/NaSCN solids shows the vibration at 2065 cm^{-1}. For LPEI/$M^{II}(SCN)_2$ (M = Co, Ni, Zn), SCN^- is dispersed as these in LPEI/NaSCN and then SCN^- does not form coordination bonds with metal ions. This indicates that metal ions are surrounded by six nitrogen atoms in LPEI.

4. ^{1}H-NMR spectra of precipitates from LPEI/$M^{II}(p\text{-TolSO}_3)_2$ (M = Co, Ni, Zn) aqueous solutions

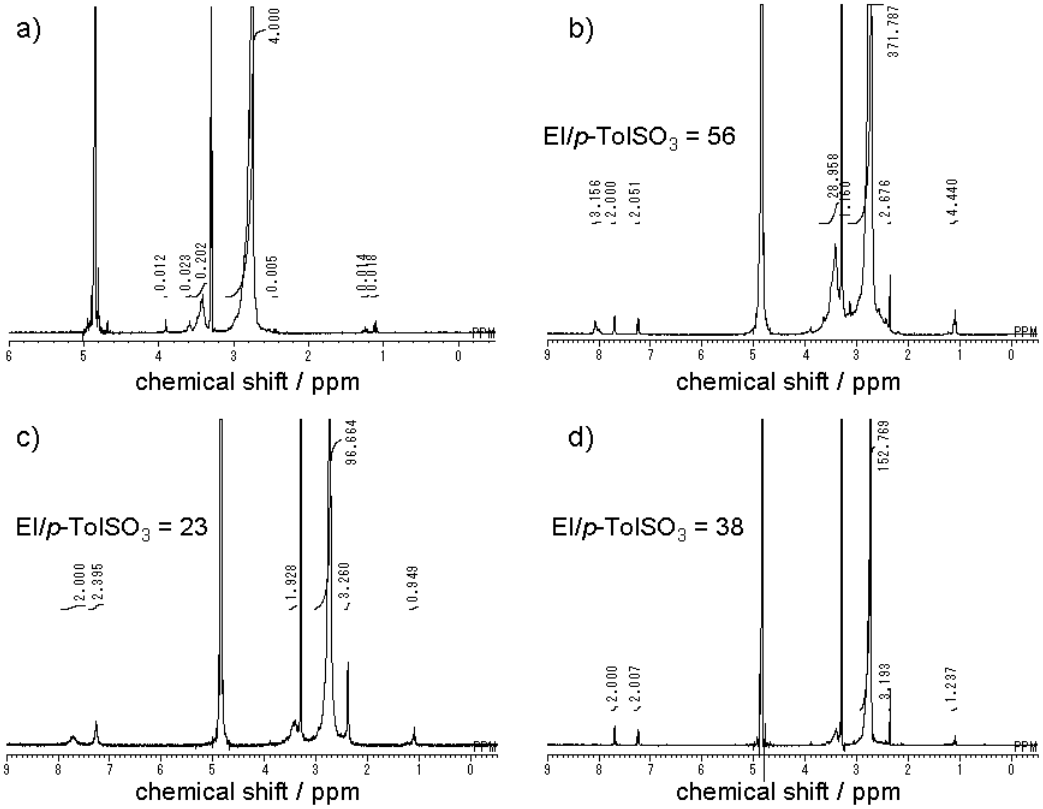

Fig. S4 ^{1}H-NMR spectra of resulting powders in CD_3OD. a) pure LPEI. b-d) the aggregates formed in LPEI aqueous solution containing divalent metal *p*-toluenesulfonate salts. Metal ions are Co (b), Ni (c), Zn (d). The proton ratios of LPEI to *p*-$TolSO_3$ (EI/*p*-$TolSO_3$) are also shown in the figures.

Figure S4 shows the ^{1}H-NMR spectra of precipitates formed from LPEI aqueous solution with/without $M^{II}(p\text{-TolSO}_3)_2$. Pure LPEI precipitates show strong signal and weak multiple signals at around 2.7 and 3.4 ppm, respectively (Figure S4a). The former arises from methylene units ($-CH_2-CH_2-$) in LPEI and the latter originates from protonated methylene moieties. On the other hand, in addition to methylene signals, LPEI precipitates formed in $M^{II}(p\text{-TolSO}_3)_2$ contained aqueous media exhibit subtle three signals at 2.4, 7.2 and 7.8 ppm (Figure S4b-d)), which are ascribed to methyl and aromatic protons of *p*-toluenesulfonate ions. Figure S4b also display multiple signals at around 8.0 ppm and the spectrum in Figure S4c appears to be broaden, which are due to the participation of paramagnetic species. These results indicate the presence of metal salts in resulting precipitates. The proton ratios of LPEI and *p*-toluenesulfonate ions (EI/*p*-$TolSO_3$) are shown in figures. These values are 23-56, that is, the ratios of EI to metal ions are 46-112. Therefore, contents of metal salts in resulting precipitates are quite smaller than those of the polymers. This suggests that metal ions play as regulators for crystallization of LPEI.

5. XRF spectra of precipitates from LPEI/$Ni^{II}X_2$ aqueous solutions

Table S1. XRF data of LPEI/Ni^{II}(*p*-$TolSO_3)_2$. Concentrations of Ni ions are 10 (a), 20 (b), 30 (c), 40 (d), 50 (e), 60 (f), 70 mM (g), respectively.

a) [Ni] = 10 mM

Element	A.W. / g mol $^{-1}$	mass%	mass% / A.W.	ratio
Si	28.09	96.40	3.432	138.0
S	32.07	2.07	0.065	2.6
Ni	58.69	1.46	0.025	1.0

b) [Ni] = 20 mM

Element	A.W. / g mol $^{-1}$	mass%	mass% / A.W.	ratio
Si	28.09	93.90	3.343	101.7
S	32.07	3.76	0.117	3.6
Ni	58.69	1.93	0.033	1.0

c) [Ni] = 30 mM

Element	A.W. / g mol $^{-1}$	mass%	mass% / A.W.	ratio
Si	28.09	92.10	3.279	67.0
S	32.07	4.99	0.156	3.2
Ni	58.69	2.87	0.049	1.0

d) [Ni] = 40 mM

Element	A.W. / g mol $^{-1}$	mass%	mass% / A.W.	ratio
Si	28.09	87.70	3.122	36.0
S	32.07	6.82	0.213	2.5
Ni	58.69	5.09	0.087	1.0

e) [Ni] = 50 mM

Element	A.W. / g mol $^{-1}$	mass%	mass% / A.W.	ratio
Si	28.09	85.50	3.044	29.7
S	32.07	8.19	0.255	2.5
Ni	58.69	6.01	0.102	1.0

f) [Ni] = 60 mM

Element	A.W. / g mol $^{-1}$	mass%	mass% / A.W.	ratio
Si	28.09	85.60	3.047	29.1
S	32.07	7.74	0.241	2.3
Ni	58.69	6.14	0.105	1.0

g) [Ni] = 70 mM

Element	A.W. / g mol $^{-1}$	mass%	mass% / A.W.	ratio
Si	28.09	81.20	2.891	21.8
S	32.07	10.70	0.334	2.5
Ni	58.69	7.78	0.133	1.0

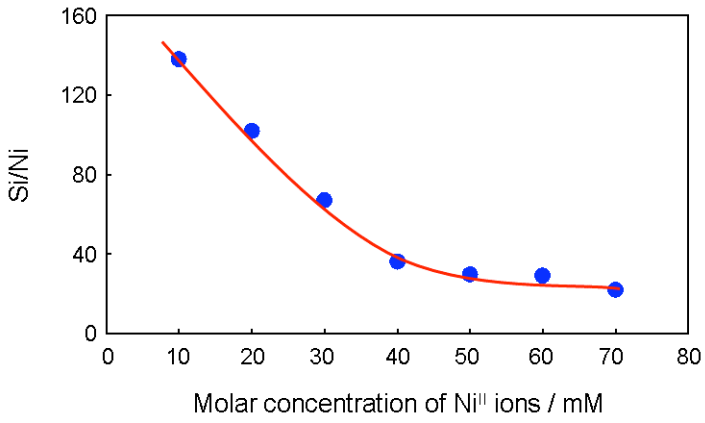

Fig. S5 Si/Ni in silica versus Ni concentration plots of LPEI/Ni^{II}(*p*-$TolSO_3)_2$. The values of Si/Ni were obtained from XRF spectra analysis of silica transcribed from LPEI/Ni^{II}(*p*-$TolSO_3)_2$ aggregates.

The XRF results of silica transcribed by LPEI precipitates from various concentrarion of Ni^{II}(*p*-$TolSO_3)_2$ aqueous solutions were summarized in Table S1 and Figure S5. From this figure, it is clear that the Si/Ni^{II} decreased linearly when the quantity of Ni^{II} added were increased up to 40 mM. Above 40 mM, the ratio seemed to become constant, indicating that similar crystal growth conditions were taken above the concentration.

6. SEM images of precipitates from LPEI/$M^{II}(p\text{-}TolSO_3)_2$ aqueous solutions

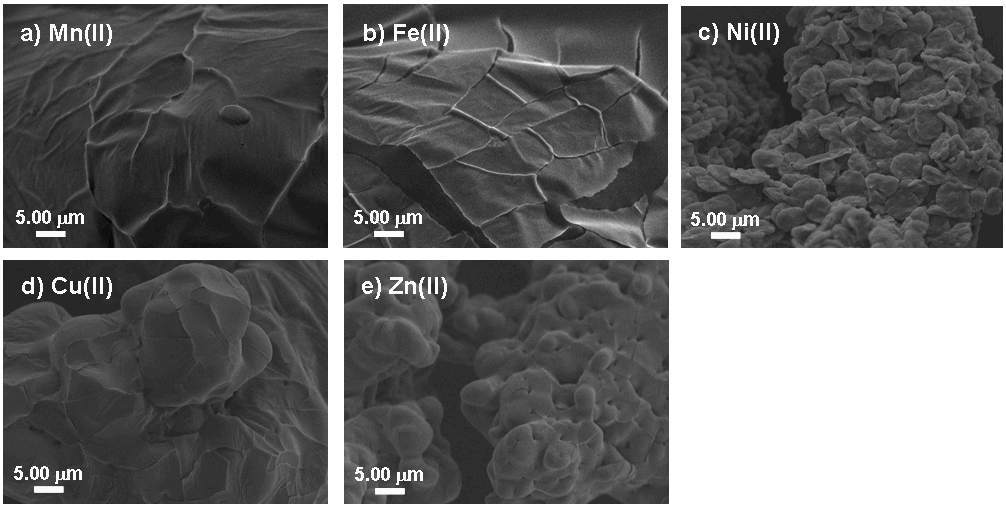

Fig. S6. SEM images of hierarchical LPEI microstructures formed in $M^{II}(p\text{-}TolSO_3)_2$ aqueous solutions. M means Mn (a), Fe (b), Ni (c), Cu (d), Zn (e). [EI] = 1000 mM, [M] = 40 mM. Samples were silicified by immersion in silica source solution (EtOH/water/MS-51 = 4/2/1 by vol.) for 30 min at r. t.

Fig. S6 show the morphologies of LPEI precipitates from metal salts aqueous solution without silicification processes. When these precipitates are dried at room temperature for SEM observation, the fibrous units of LPEI precipitates have a tendency to associate each others and finally the hierarchical structures disappear as shown in Fig. S6. We can observe barely the simulacra of hierarchy of LPEI precipitates from $Ni(p\text{-}TolSO_3)_2$ aq (Fig. S6 c)).

7. SEM images of silica transcribed by LPEI precipitates from $M^{II}(p\text{-}TolSO_3)_2$ aqueous solutions

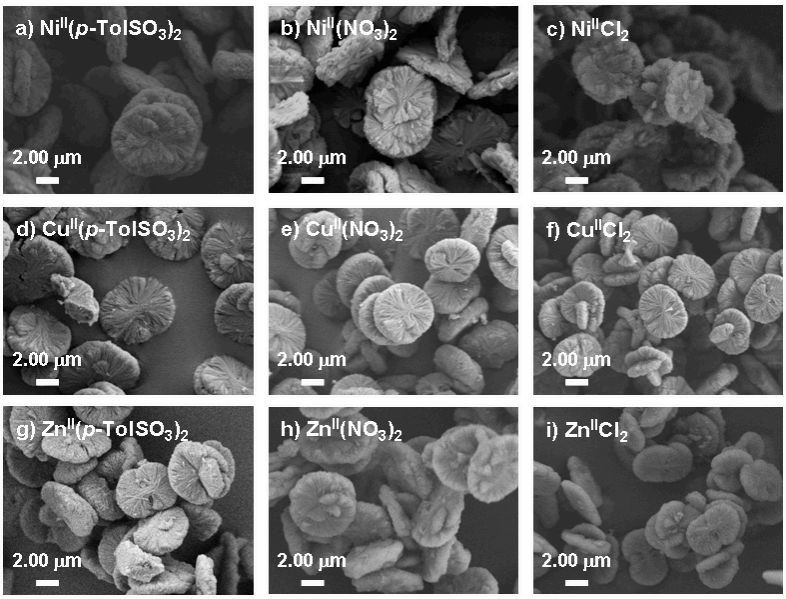

Fig. S7 SEM images of hierarchical silica transcribed by LPEI precipitates which are altered in the presence of $M^{II}X_2$ under the conditions with [EI] = 1000 mM, [M] = 60 mM. $M^{II}X_2$: $Ni^{II}(p\text{-}TolSO_3)_2$ (a), $Ni^{II}(NO_3)_2$ (b), $Ni^{II}Cl_2$ (c), $Cu^{II}(p\text{-}TolSO_3)_2$ (d), $Cu^{II}(NO_3)_2$ (e), $Cu^{II}Cl_2$ (f), $Zn^{II}(p\text{-}TolSO_3)_2$ (g), $Zn^{II}(NO_3)_2$ (h) and $Zn^{II}Cl_2$ (i). All the silica particulates were obtained by immersion the precipitates in silica source solution (EtOH/water/TMOS = 2/1/1 by vol.) for 60 min at r. t.

8. EPR spectra of silica transcribed by LPEI precipitates

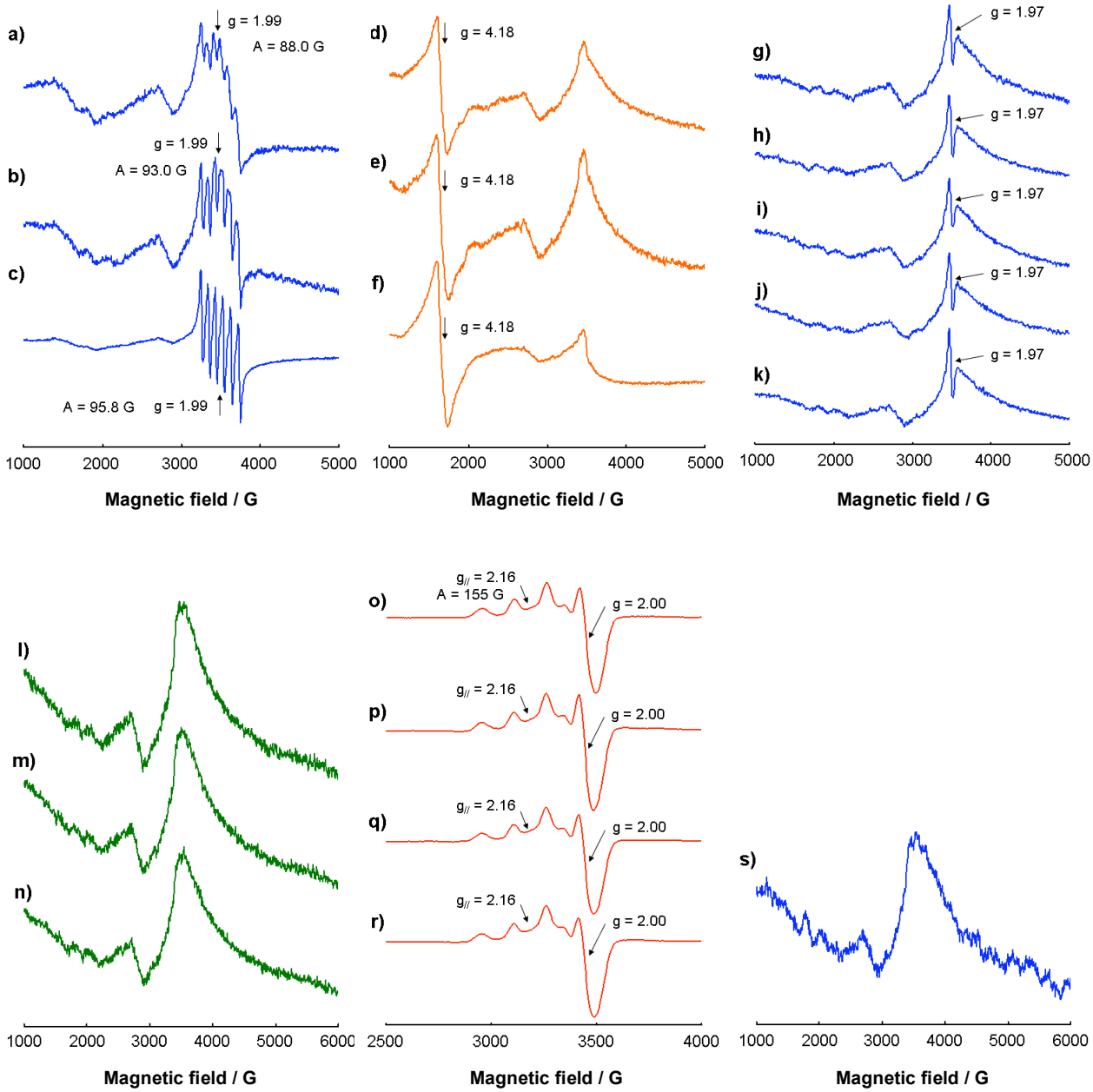

Fig. S8. EPR spectra (X-band) of hierarchical silica microstructures which are transcribed LPEI precipitates from water containing $M^{II}X_2$ salts. (a) Mn(*p*-TolSO$_3$)$_2$. (b) Mn(NO$_3$)$_2$. (c) MnCl$_2$. (d) Fe(*p*-TolSO$_3$)$_2$. (e) Fe(BF$_4$)$_2$. (f) FeCl$_2$. (g) Co(*p*-TolSO$_3$)$_2$. (h) Co(BF$_4$)$_2$. (i) Co(NO$_3$)$_2$. (j) CoCl$_2$. (k) Co(NCS)$_2$. (l) Ni(*p*-TolSO$_3$)$_2$. (m) Ni(NO$_3$)$_2$. (n) NiCl$_2$. (o) Cu(*p*-TolSO$_3$)$_2$. (p) Cu(BF$_4$)$_2$. (q) Cu(NO$_3$)$_2$. (r) CuCl$_2$. [EI] = 1000 mM, [M] = 40 mM. Silica transcribed from LPEI precipitates from water without metal salts was measured for comparison (f). Applied frequencies were 9.639 for a, g-l, k-m, p, r) or 9.644 GHz for b-f, j, n, o, q, s) and spectra were recorded at room temperature. All LPEI precipitates were silicified by immersion in silica source solution (EtOH/water/MS-51 = 4/2/1 by vol.) for 30 min at r. t.

Fig. S8 shows EPR spectra at room temperature of silica transcribed from LPEI precipitates from metal salts. In spite of differences of counter anions, spectra of same metal ions are almost same, which suggest that metal ions are surrounded amine units of LPEI. In Fig. S8 a) - c), well-resolved

sextet signals centered at g = 1.99 with a hyperfine splitting constant (A) of 88-96 G are observed, which are characteristic for Mn(II) complexes with O_h environments.[3] Fig. S8 d) - f) show the signals at 1650 G (g = 4.18) and at 2700-3500 G. The former is ascribed to Fe(III) ions in low six-coordinated symmetry. It is reasonable that some parts of Fe(II) ions were oxidized to Fe(III) ions during complexation with LPEI. The latter is also observed in Fig. S8 l) - n) and s). Therefore, the signals at around 3500 G are likely to originate from silica and/or LPEI. Fig. S8 g) - k) exhibit sharp signals centered at g = 1.97 and the signals would be caused by highly symmetric T_d Co(II) ions.[3] Generally, Co(II) ions surrounded by amine ligands tend to be oxidized and then adopt stable O_h coordination environments. Therefore, in our systems, Co(II) ions in T_d symmetry might be due to concomitant encapsulation of dissolving Co(II) salts in silica matrix during silica deposition. Fig. S8 o) - r) show the typical EPR signals for Cu(II) ions.[3, 4] Because of the measurements at ambient temperature, we can not discuss clearly the coordination states of Cu(II) ions. However, taking into account of low $g_{//}$ values ($g_{//}$ = 2.16), Cu(II) centers are not significantly distorted and then O_h might be taken.[5, 6]

References

1. (a) C. K. Jørgensen, *Acta*. *Chem*. *Scand*., 1956, **10**, 887; (b) H. B. Jonassen, B. E. Douglas, *J*. *Am*. *Chem*. *Soc*., 1949, **71**, 4094.
2. H. Zhang, J. Wang, H. Zheng, K. Zhuo, Y. Zhao, *J*. *Phys*. *Chem*. *B*, 2005, **109**, 2610.
3. J. Evans, A. B. Zaki, M. Y. EI-Sheikh, S. A. EI-Safty, *J*. *Phys*. *Chem*. *B*, 2000, **104**, 10271.
4. C. F. G. C. Geraldes, M. P. M. Marques, B. de Castro, E. Pereira, *Eur*. *J*. *Inorg*. *Chem*., 2000, 559.
5. B. Bleaney, K. D. Bowers, D. J. E. Ingram, *Proc*. *R*. *Soc*., 1955, **A228**, 147
6. S. Zhu, F. Kou, H. Lin, C. Lin, M. Lin, Y. Chen, *Inorg*. *Chem*., 1996, **35**, 5851.